Catalysis Science & Technology

Accepted Manuscript

ROYAL SOCIETY OF CHEMISTRY

www.rsc.org/catalysis

Catalysis Science & Technology

ARTICLE

Mechanistic Insights into Selective Hydrodeoxygenation of Lignin Derived β-O-4 Linkage to Aromatic Hydrocarbons in Water

Received 00th xx 20xx,
Accepted 00th xx 20xx

DOI: 10.1039/x0xx00000x
www.rsc.org/

Zhicheng Luo,[a] Chen Zhao*[a]

The route for selective hydrodeoxygenation of phenethoxybenzene (PEB, represents the dominant β-O-4 linkage in lignin) to produce benzene and ethyl-benzene is realized by a multi-functional Ru/sulfate zirconium (Ru/SZ) catalyst in aqueous phase. One-pot hydrodeoxygenation of PEB is initially cleaved at forming C_6 phenol and C_8 ethyl-benzene via the selective cleavage route of $C_{aliphatic}$-O bond (k_1). While the C_8 ethyl-benzene is stable against further hydrogenation under the selected condition, the C_6 phenol intermediate is hydrogenated to cyclohexanol with a rapid rate (k_2), and the sequential steps of cyclohexanol dehydration (k_3) as well as cyclohexene dehydrogenation (k_4) leads to the target benzene formation. A high temperature (240 °C) together with low hydrogen pressure (8 bar) is essential for achieving such specific route, suppressing the side-reactions of aromatics hydrogenation. Compared to Ru/SZ, Pd/SZ catalyzes the high rate for cleaving of ether (k_1), but fails in sequential C_6 phenol hydrogenation (k_2) and cyclohexanol dehydration (k_3), and thus is not able to accomplish the complex cascade reaction. Pt/SZ performs poorly in the primary step of ether cleavage (k_1), and therefore, blocks the following sequential steps. The separate kinetics tests on phenol and cyclohexanol hydrodeoxygenation reveal that benzene is not produced by the direct hydrogenolysis, but by the dehydration-dehydrogenation route. The high benzene yield from phenol is probably attributed to few surface adsorbed H· species reserved on Ru/SZ during phenol hydrodeoxygenation, as evidenced by the model reaction of cyclooctene hydrogenation with the used Ru/SZ in presence of N_2.

Introduction

Lignin is a natural bio-polymer with methoxylated C_9 phenyl-propane units in a three-dimensional structure that is randomly connected by C-C and C-O linkages, contributing to the valuable bio-resource that is rich in aromatics-rings with high energy-density.[1] Selective cleavage of C-O bond of lignin linkage is a critical step for lignin depolymerization. The most abundant C-O linkage in lignin is β-O-4 (45-50%),[2] and thus, it is frequently selected as the starting material to investigate the mechanism for cleavage of the main ether linkage in lignin.

The β-O-4 ether bond is connected by one part of $C_{aliphatic}$-O bond (bond dissociation energy: ca. 289 kJ·mol^{-1}) and another part of $C_{aromatic}$-O bond (bond dissociation energy: ca. 314 kJ·mol-1).[3] Such ether bond can be cleaved by the main approaches of pyrolysis, hydrolysis, and hydrogenolysis.[4] Because of the relatively much weaker dissociation energy of the $C_{aliphatic}$-O bond, substituted phenol and ethyl-benzene compounds are more inclined to be generated.

Hydrolysis with acid is considered to be a solution to break down the β-O-4 linkages. For example, HCl released hydrolysate compounds from β-O-4 linkage in the dioxane-water mixture.[5] Moreover, an acidic ionic liquid, 1-H-3-methylimidazolium chloride, showed high efficiency to hydrolyze the β-O-4 linkage with an exceeding 70% yield.[6] Besides, the pyrolysis route can also break down the C-O bond.[7] The pyrolysis reaction is majorly involved into free-radical reactions, molecular rearrangements, and concerted eliminations, and thus is shown to be very complex. Such thermal decomposition of the β-O-4 sub-structure by pyrolysis preferentially produced a mixture majorly consisting of styrene and phenolic compounds at 300-400 °C.[8]

Apart from the hydrolysis and pyrolysis routes, the cleavage of β-O-4 ether bond can be accomplished on metal-catalyzed hydrogenolysis in the liquid phase. The homogeneous catalysts including Ni[9], Co[10], and Ru[11] complexes showed high selectivity in cleaving of the $C_{aliphatic}$-O bond of β-O-4 compounds to produce corresponding aromatic and phenolic compounds in relatively mild conditions. Furthermore,

[a] *Shanghai Key Laboratory of Green Chemistry and Chemical Processes, School of Chemistry and Molecular Engineering, East China Normal University, Shanghai 200062, China.*
E-mail: czhao@chem.ecnu.edu.cn
Electronic Supplementary Information (ESI) available: [details of any supplementary information available should be included here]. See DOI: 10.1039/x0xx00000x

ARTICLE

the unsupported nanoparticles Fe[12], RuNi[13a], and AuNi[13b] also exhibited high activities in scission of the C-O bonds of the β-O-4 linkage. With respect to more applicable issues of catalyst recovery and cost, the heterogeneous Ni/SiO_2 catalyst [14] manifested good activity in cleaving of the $C_{aliphatic}$–O bond of the β-O-4 linkage to ethyl-benzene and cyclohexanol in water. Combined Ni with HZSM-5 in presence of hydrogen,[15] the cleaved cyclohexanol intermediate was in turn dehydrated and hydrogenated to cyclohexane, while the other cleaved ethyl-benzene intermediate was hydrogenated to ethyl-cyclohexane. Analogous bifunctional catalysts with metal and acid sites can also quantitatively hydrodeoxygenate such ether compounds to cyclic alkanes at similar conditions.[16] The FeMoP catalyst selectively hydro-deoxygenated of the β-O-4 model compound to aromatics at a high temperature of 400 °C in presence of 2.1 MPa H_2 in decane.[17]

However, the biomass raw resource contains substantial amounts of water and the target aromatic hydrocarbons products are more valuable than the cyclic alkanes in the viewpoint of industrial application. To produce aromatic hydrocarbon in water, recently it is reported that in the neat aqueous phase an aryl ether mixture derived from lignin is selectively cleaved and hydrodeoxygenated to C_6-C_9 aromatic hydrocarbons.[18,19] Here, in this contribution we explore the comparison of three metals of Pd, Pt, and Ru for selectively cleaving and deoxygenating of the C-O bond of phenethoxybenzene ether (PEB, β-O-4 model compound) via the kinetics study. The subtly controlling of reaction route is shown to be manipulated by coordinating inter-coupling influence factors of metal sites, acid sites, hydrogen pressures, as well as temperatures, in order to realize a delicately designed catalytic system for forming benzene and ethyl-benzene from PEB in aqueous phase. Furthermore, the involved key individual steps including phenol and cyclohexanol conversion in the overall PEB hydrodeoxygenation process are explored and compared in details.

Results and discussion

Catalyst characterization

Table 1. Characterization of the supported metal (Ru, Pd, Pt) catalysts.

Cat.	S_{BET} ($m^2 \cdot g^{-1}$) [a]	D_{metal} (%) [b]	$d_{CO\text{-}chem}$ (nm) [c]	Acid density ($mmol \cdot g^{-1}$) [d]
Ru/C	924	36	3.1	-
Pd/C	1100	36	3.1	-
Pt/C	1080	21	5.2	-
Ru/SZ	21	21	5.2	0.11
Pd/SZ	21	27	4.1	0.43
Pt/SZ	16	28	3.9	0.55

[a] Detected by N_2 sorption.
[b] Determined by CO chemisorption measurement.
[c] Analyzed by the equation $d = 1.1/D_{metal}$.
[d] Measured by temperature programmed desorption of NH_3.

The physic-chemical properties of the carbon and sulfate zirconia (SZ) supported Ru, Pd, Pt metal catalysts are compiled in Table 1. The three metals were incorporated into the carbon and SZ supports by the HCHO liquid reduction method. According to the nitrogen sorption data, the BET specific surface areas of the carbon supported metal catalysts (Ru/C, Pd/C, Pt/C) were estimated to be 924-1100 $m^2 \cdot g^{-1}$, while the BET-specific surface areas of the Ru/SZ, Pd/SZ, Pt/SZ catalysts were around 20 $m^2 \cdot g^{-1}$. Determined from the CO chemisorption measurements, the metal dispersions of these catalysts were listed in Table 1, ranging from 21% to 36%. Based on the empirical formula (d = 1.1/D_{metal}), the particle sizes of Ru, Pd, Pt were shown to be 3.0-5.2 nm. The temperature programmed desorption of ammonia (NH_3-TPD) profile revealed that the acid concentrations of Pd/SZ (0.43 $mmol \cdot g^{-1}$) and Pt/SZ (0.55 $mmol \cdot g^{-1}$) was much higher than that of Ru/SZ (0.11 $mmol \cdot g^{-1}$), indicating that the stronger interaction between Ru and SZ leads to the higher reduction of the active acid sites. The selected Ru/SZ catalyst in the present work exhibited granulated and inhomogeneous shape with a crystal size of around 1-10 μm, shown from the SEM image (see Fig. S1). In addition, the Ru, Pd, Pt nanoparticles on SZ were around 2.0 ± 0.4, 3.9 ± 0.6, 3.7 ± 0.5 nm, as observed from the TEM images (see Fig. S2).

Selective hydrodeoxygenation of PEB to aromatic hydrocarbons

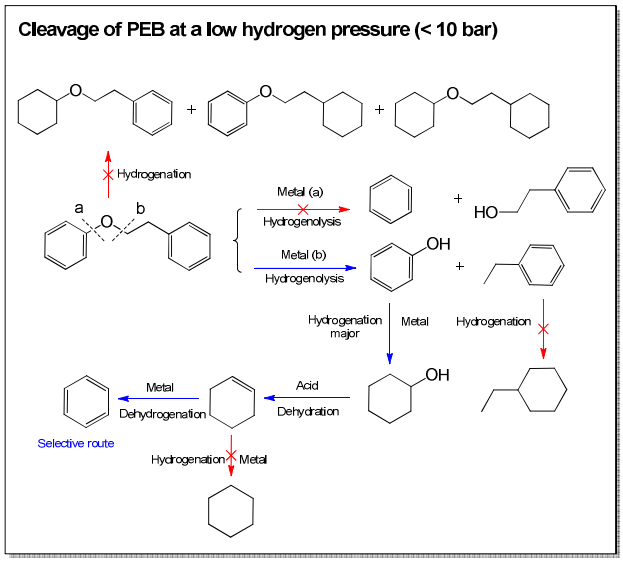

Scheme 1. The dedicatedly designed reaction routes for selective hydrodeoxygenation of PEB to C_6 benzene and C_8 ethyl-benzene in the aqueous phase.

A specific route for HDO of PEB to benzene and ethyl-benzene is designed in the blue lines of Scheme 1. It is considered that the key factors for realizing the designed pathways include the following points: 1) selective hydrogenolysis of ether at position b for producing phenol and

ethyl-benzene, 2) the full blockage of the hydrogenation routes on benzene-ring compounds comprising of PEB, ethyl-benzene, and cyclohexene to form saturated alkanes (the red lines in Scheme 1), 3) the faster hydrogenation rate of phenol than that of ethyl-benzene, and subsequently, the hydrogenated product cyclohexanol is sequentially dehydrated and dehydrogenated to benzene.

Different influence factors including metal sites, acid sites, hydrogen pressures, and temperatures will be then subtly investigated to manipulate the exclusive path of selective cleavage of $C_{aliphatic}$-O of PEB, as well as coordinate the individual cascade steps of phenol hydrogenation, cyclohexanol dehydration, and cyclohexene dehydrogenation to generate the maximum aromatic hydrocarbons.

Selection of proper metal center for cleaving of the C-O bond of PEB in water

The β-O-4 linkage is the most abundant connection units (around 50%) in lignin,[1] and thus, phenethoxybenzene ether (PEB) is selected as its representative model compound to investigate the reaction pathways of ether scission. In principle, the C-O bond can be cleaved by routes of hydrogenolysis, hydrolysis, or multi-combinations (see Scheme 1). Concerning on the hydrolysis of PEB at 240 °C for 1 h in aqueous phase, a variety of solid acids such as -SO_3H solid acids and Si-Al zeolites were employed for testing (see Table 2). The results manifested that all the selected catalysts were inactive for hydrolysis of PEB, suggesting the C-O bond of aryl ether was quite inert with solid acids in the high-temperature water. With activated carbon, the conversion of PEB was zero at selected conditions. However, when metals catalysts such as Ru/C, Pd/C, and Pt/C were used, the ether cleavage yield (including C_6 and C_8 fragments from PEB) was sharply increased to respective 97%, 91%, and 49% at identical conditions (see Table 2). In a second step, these three metals (Ru/C, Pd/C, and Pt/C) are comparatively studied sequentially.

Table 2. Cleavage of PEB with solid acids and metal catalysts in aqueous phase.[a]

-SO_3H Solid acid	Cleaved yield (%)	Si-Al solid acids	Cleaved yield (%)	Catalyst	Cleaved yield (%)
Nafion	0	HZSM-5	0	Ru/C	97
Amberlyst	0	HBeta	0	Pd/C	91
Sulfate Zirconium	0	HY	0	Pt/C	49

[a] General conditions: PEB (1.0 g), solid acid or metal catalyst (0.10 g), H_2O (100 mL), 240 °C, 8 bar H_2, 1 h, stirring at 650 rpm.

Subsequently the kinetics of PEB conversion was performed over three metals at a relatively high temperature of 240 °C in presence of 8 bar H_2 (see Fig. 1). The kinetic results showed that both Ru/C and Pd/C can catalyze high C-O bond cleavage rates on PEB (165 and 270 mmol·g^{-1}·h^{-1}, respectively, see Table 3), but Pd/C led to a much higher partial benzene ring hydrogenation rate (47 mmol·g^{-1}·h^{-1}) than Ru/C (3.3 mmol·g^{-1}·h^{-1}), implying that Ru/C is more capable for selectively cleaving of the C-O bonds of PEB. In accordance to the activity test influenced by the temperature, Pt/C performed poorly for both C-O bond cleavage and benzene ring hydrogenation, with respective slow rates of 47 and 26 mmol·g^{-1}·h^{-1}. Through the comparison of hydrogenolysis and hydrogenation rates (Table 3), Ru/C is more selective for breaking down the C-O bond of PEB by hydrogenolysis.

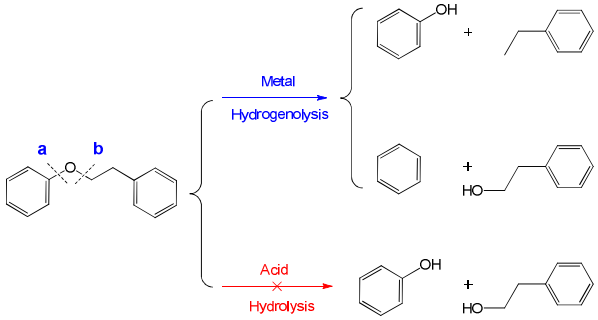

Scheme 2. The plausible pathways for cleaving of the C-O bond of PEB in water.

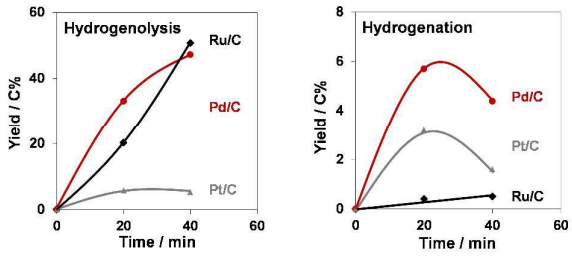

Figure 1. Comparison of hydrogenolysis and hydrogenation of PEB over Ru/C, Pt/C, and Pd/C (5 wt.%, 0.020 g). Hydrogenolysis products includes C_6 and C_8 fragments, and hydrogenation products includes partial benzene-ring hydrogenated C_{14} ether. The detailed product analysis was listed in Table S1. General conditions: PEB (1.0 g), H_2O (100 mL), 240 °C, 8 bar H_2, stirring at 650 rpm.

Table 3. Data for Ru/C, Pd/C, Pt/C catalyzed individual rates in PEB conversion.

Cat.	Initial C-O bond cleavage rate (mmol·g^{-1}·h^{-1})	Initial partial hydrogenation rate (mmol·g^{-1}·h^{-1})	Hydrogenolysis/ hydrogenation rate ratio
Ru/C	165	3.3	55
Pd/C	270	47	5.7
Pt/C	47	26	1.8

The initial rates for C-O bond cleavage and partial hydrogenation were calculated from the curves of hydrogenation and hydrogenolysis performances in Fig. 1. General condition: PEB (1.0 g), metal catalyst (5 wt%, 0.02 g), H_2O (100 mL), 240 °C, 8 bar H_2, stirring at 650 rpm.

ARTICLE

Manipulating the ether cleavage pathways of PEB conversion via the variation of temperatures and hydrogen pressures

With three metal Ru/C, Pd/C, and Pt/C catalysts (5 wt%, synthesized by liquid-phase HCHO reduction), the influence of temperatures (ranging from 180 °C to 240 °C) was explored towards PEB hydrodeoxygenation over Ru/C (see Figs. 2a-2c). The cleavage reaction on PEB was performed in an aqueous phase in a stirred Parr autoclave in presence of 8 bar H_2. With an increasing temperature, the C-O cleavage yields of PEB were enhanced from 77% to 97% over Ru/C accordingly (Fig. 2a). The co-presence of C_8 phenyl-ethanol (yield: 15%) and ethyl-benzene (yield: 30%) over Ru/C at 180 °C suggests that the C-O bond can be cleaved at position a ($C_{aromatic}$-O) or b ($C_{aliphatic}$-O) of PEB (see Scheme 1). An increase of temperature up to 240 °C led to selective C_6 phenol and C_8 ethyl-benzene formation, as Ru catalyzes the exclusive route for cleaving of $C_{aliphatic}$-O bond of PEB (at position b), due to the much lower bond energy of $C_{aliphatic}$-O (289 $kJ{\cdot}mol^{-1}$) than $C_{aromatic}$-O (314 $kJ{\cdot}mol^{-1}$)[3]. In addition, C_6 phenol was slightly enhanced from 22% to 28% with a rising temperature (from 180 °C to 240 °C), while the yields of other C_6 products including cyclohexanone/ol and benzene/cyclohexane were stable at respective 8% and 5%. The partial and full hydrogenation products from PEB (with a yield around 20%) appeared at a low temperature of 180 °C, whereas they gradually decreased to 2% as the temperature increased up to 240 °C.

In comparison to Ru/C, Pd/C led to an increasing C-O cleavage yield from 53% (180 °C) to 91% (240 °C) as well (Fig. S2), implying that Pd is capable for cutting down the C-O bond of PEB. In a similar way, the C_8 phenyl-ethanol yield was decreased from 25% (at 180 °C) to 2% (at 240 °C). However, only the C_6 fragment of phenol and cyclohexanone/ cyclohexanol was observed, without any benzene or cyclohexane detected at such temperature range. Meanwhile, unlike Ru/C, Pd/C led to higher concentrations of (partial and full) hydrogenation products (from 32.1% at 180 °C to 7.7% at 240 °C) during temperature variations.

The third metal Pt/C catalyzed the increasing C-O cleavage yields from 9% to 51% with a rising temperature (Fig. S2). However, the activity was far below those with Ru/C and Pd/C catalysts at identical condition. Pt/C generated the selective products of C_6 phenol (17% yield) and C_8 ethyl-benzene (27% yield) at 240 °C, suggesting that the $C_{aliphatic}$-O bond was dominantly cleaved when the temperature arose.

Based on these results, it can be generally concluded that at the selected temperature range Ru/C and Pd/C catalysts manifest superior activities than Pt/C in cleaving of the C-O ether bond of PEB. The dominant products of ethyl-benzene and phenol derivatives at 240 °C demonstrate that the $C_{aliphatic}$-O bond is selectively cleaved as temperatures increase. Moreover, the partial benzene-ring hydrogenation products gradually decrease as a function of temperature, indicating that hydrogenolysis but not hydrogenation plays a major role when temperature rises up.

Focused on Ru/C, the influence of H_2 pressure towards the reaction pathway of PEB was explored (shown at Fig. 2d-2f). In relative low H_2 pressure ($\leq$ 10 bar), PEB was selectively cleaved at $C_{aliphatic}$-O position to produce C_6 phenol and C_8 ethyl-benzene. Between them, C_6 phenol was partially converted to cyclohexanol and cyclohexanone, while C_8 ethyl-benzene was unchanged. On increasing H_2 pressure from 20 to 30 bar, reaction pathways were altered to three directions, hydrogenolysis at position b ($C_{aliphatic}$-O) still dominated with the corresponding cleavage yields decreasing from 95% to 80%. Moreover, with the increasing hydrogen pressure the yields of phenyl-ethanol increased from 5% to 9%, indicating that relative high concentration of hydrogen would contribute to the scission of $C_{aromatic}$-O at position a for producing C_6 benzene and C_8 phenyl ethanol. The hydrogenation yields of PEB increased from 3.7% to 20%, suggesting that the relative high hydrogen pressure favors for enhancing the proportion of hydrogenation to hydrogenolysis. Therefore, the high hydrogen pressure leads to complicated and unselective products, and in order to construct a selective $C_{aliphatic}$-O bond cleavage route, a relatively low H_2 pressure (ca. 8 bar) is adopted.

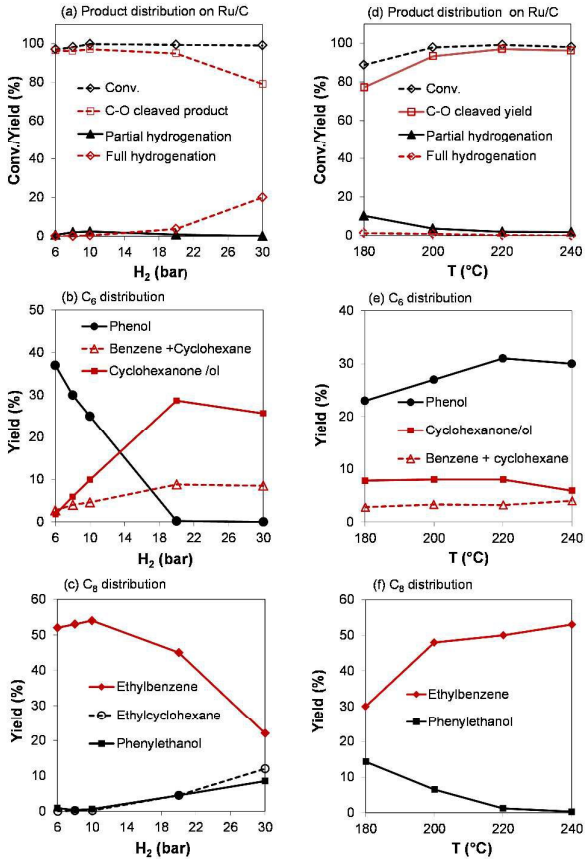

Figure 2. Product distributions on PEB conversion over Ru/C in aqueous phase as a function of temperature (a-c) and hydrogen pressure (d-f). Reaction conditions: PEB (1.0 g), Ru/C (5 wt%, 0.10 g), 240 °C, H_2O (100 mL), 1 h, stirring at 650 rpm.

Understanding the individual steps involved into selective hydrodeoxygenation of PEB to aromatic hydrocarbons

To understand the intrinsic reaction mechanism, kinetics of PEB conversion was conducted with Ru/C at optimized conditions (240 °C, 8 bar H_2) (see Fig. 3a). The kinetic curve showed that PEB was selectively cleaved to C_6 phenol and C_8 ethyl-benzene (100% selectivity) in the beginning. By contrast, it did not produce any products of partial hydrogenation, full hydrogenation, and cleaved products of C_6 benzene and C_8 phenyl ethanol. This means that Ru catalyzes the single route for cleaving of the C-O bond of PEB at position b ($C_{aliphatic}$-O bond) at optimized conditions, while completely supressing the plausible pathways of hydrogenation of benzene rings together with hydrogenolysis at position a ($C_{aromatic}$-O bond). As a function of time, the intermediate phenol was swiftly converted to cyclohexanone and cyclohexanol over Ru/C.

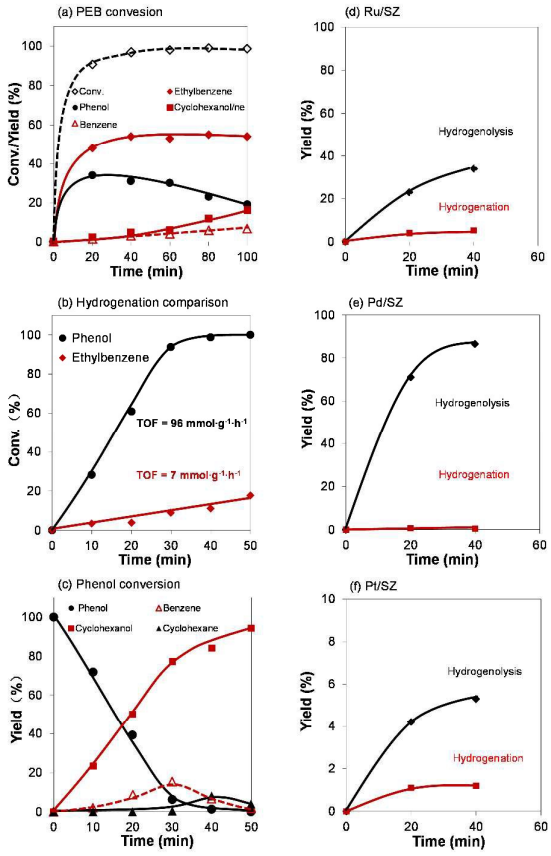

Figure 3. (a) Product distributions for conversion of PEB over Ru/C, and (b) Comparison of phenol and ethyl-benzene hydrogenation, (c) kinetic curves of phenol hydrogenation over Ru/C in aqueous phase. Kinetics of PEB conversion with SZ supported metal catalysts (d) Ru/SZ, (e) Pd/SZ, and (f) Pt/SZ. General condition: Ru/C (0.1 g), H_2O (100 mL), 240 °C, 8 bar H_2, stirring at 650 rpm, (a) PEB (1.0 g), (b) phenol (0.5 g) and ethyl-benzene (0.5 g), (c) phenol (0.5 g). In figures (3d) (3e) (3f), Ru/SZ, Pd/SZ, and Pt/SZ (0.020 g) catalysts and PEB (1.0 g) were used.

It can be found that phenol was hydrogenated with a rapid rate while ethyl-benzene was very stable at selected system. To clarify it, in a separate experiment by co-introduction of phenol and ethyl-benzene over Ru/C at 240 °C in presence of H_2, the kinetic result demonstrated that phenol catalyzed a high hydrogenation rate of 96 mmol·g^{-1}·h^{-1}, while by comparison, the ethyl-benzene hydrogenation only attained a slow rate of 7 mmol·g^{-1}·h^{-1} (Fig. 3b). Such rate disparity leads to a fast phenol hydrogenation while ethyl-benzene was almost unchanged at identical conditions.

The separate kinetics of phenol hydrogenation (Fig. 3c) revealed that the primary product was cyclohexanol over Ru/C within same conditions. To achieve target benzene formation from phenol intermediate, our further strategy was designed as sequential dehydration of cyclohexanol, and afterwards selective dehydrogenation of cyclohexene to benzene with a subtle Ru/acid bifunctional catalyst at an appropriate condition.

Concerning on the acceleration step of cyclohexanol dehydration, sulfate zirconia (SZ) is introduced as the metal support to construct the bifunctional catalyst (Figs. 3d-3f). In general, acid promotes the hydrogenolysis rate especially for Pd, in which Pd/SZ enhanced the cleavage rate from 270 mmol·g^{-1}·h^{-1} to 578 mmol·g^{-1}·h^{-1} (Table 4). The obtained rate results (see Table 4) illuminated that Ru/SZ and Pd/SZ are both active for the primary C-O bond cleavage (k_1 = 178 and 578 mmol·g^{-1}·h^{-1}, respectively), whereas Pt/SZ seems to be still inactive (k_1 = 34 mmol·g^{-1}·h^{-1}). The total catalytic trend over metal/SZ is as similar as the carbon supported metal catalysts.

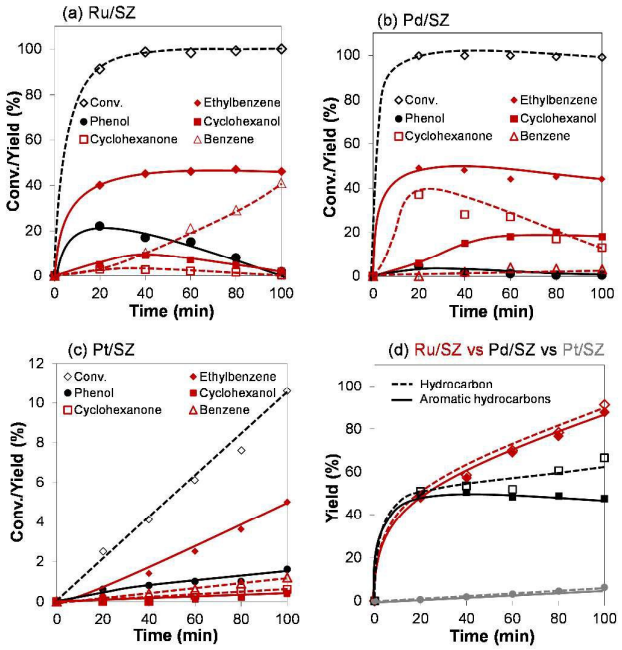

Figure 4. Product distributions of BPE conversion over (a) Ru/SZ, (b) Pd/SZ, (c) Pt/SZ, (d) Ru/SZ vs Pd/SZ vs Pt/SZ in water as a function of time. Reaction conditions: BPE (1.0 g), Ru/SZ, Pd/SZ, Pt/SZ (5 wt%, 0.10 g), 240 °C, H_2 (8 bar), H_2O (100 mL), stirring at 650 rpm.

ARTICLE

Table 4. Data for Ru/SZ, Pd/SZ, and Pt/SZ catalyzed individual rates during PEB conversion.

Catalyst	Initial C-O bond cleavage rate ($mmol \cdot g^{-1} \cdot h^{-1}$)	Initial partial hydrogenation rate ($mmol \cdot g^{-1} \cdot h^{-1}$)
Ru/SZ	188	32
Pd/SZ	578	5.7
Pt/SZ	34	9.0

General condition: PEB (1.0 g), metal/SZ catalyst (5 wt%, 0.02 g), H_2O (100 mL), 240 °C, 8 bar H_2, stirring at 650 rpm. The rates are calculated on the basis of Figs. 4a-4c.

To compare and explore the individual steps in the cascade hydrodeoxygenation reaction, kinetics of PEB conversion with three metals was conducted afterwards. It plotted that in an initial time, PEB was selectively cleaved to C_6 phenol and C_8 ethyl-benzene with nearly 100% selectivity on three metals (see Figs. 4a-4c). In line with the high initial rates on C-O bond cleavage of PEB, Ru/SZ and Pd/SZ both attained high conversion values (exceeding 90%) in 20 min., while Pt/SZ merely reached a conversion of 3% at the same condition (Fig. 4c). As a function of time the total amount of aromatics was achieved at stable 50% on Pd/SZ, however, the aromatic yield on Ru/SZ was linearly increased to 90% at 100 min.. In should be addressed that the C_8 product ethyl-benzene was almost unchanged at keeping 50% yield over Pd/SZ or Ru/SZ during the conversion, implying that Pd/C (total aromatics yield: 50%) is not able to generate any aromatics from the C_6 fragment.

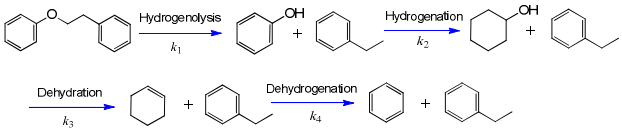

Scheme 3. Simplified reaction steps in HDO of PEB to C_6 benzene and C_8 ethyl-benzene.

Exploring into the reaction pathway of converting C_6 phenol intermediate on Pd/SZ (Scheme 3), it was observed that cyclohexanone was converted to cyclohexanol in a relatively slow rate, which led to a very small k_2 value to cyclohexanol formation and then blocked the sequential cyclohexanol dehydration step on SZ (k_3), consequently the target product benzene was impeded (Fig. 4b). By contrast, the phenol intermediate was swiftly converted to cyclohexanol (k_2) on Ru/SZ, and thus sequential steps of dehydration of cyclohexanol to produce cyclohexene (k_3) and dehydrogenation of cyclohexene to form benzene (k_4) were favourable on Ru/SZ towards the total cascade hydrodeoxygenation reaction (Fig. 4a). With respect to Pt/SZ, it catalyzed the slow rate in the primary step of C-O bond cleavage (k_1, Fig. 4c), and therefore, the following tandem steps (k_2, k_3, and k_4) were suppressed and blocked (Fig. 4c). The influence of metal center (SZ as support) towards the individual steps in HDO of PEB to aromatics was summarized at Table 5, that is, Ru favored the whole sequential and integrated steps of k_1, k_2, k_3, and k_4, while Pd hindered the crucial step k_2 and Pt blocked the primary step k_1. Consequently Ru/SZ performed excellently throughout the four steps for forming target aromatics in the integrated HDO process (Fig. 4d).

Table 5. Metal center influences individual steps in PEB hydrodeoxygenation to aromatics

Metal	k_1	k_2	k_3	k_4
Ru/SZ[a]	+	+	+	+
Pd/SZ	+	-	n.d.	n.d.
Pt/SZ	-	-	n.d.	n.d.

+: favored, -: not favored; n.d.: not determined.

k_1: C-O bond cleavage rate of PEB

k_2: Phenol hydrogenation rate to cyclohexanol

k_3: Cyclohexanol dehydration rate to cyclohexene

k_4: Cyclohexene dehydrogenation rate to benzene

In summary, the overall route for the precise hydrodeoxygenation of PEB to C_6 benzene and C_8 ethyl-benzene aromatic hydrocarbons is depicted at Scheme 1 (blue lines). The C-O bond of PEB is initially cleaved at $C_{aliphatic}$-O bond to form phenol and ethyl-benzene. The resulted C_8 ethyl-benzene is stable, while the other C_6 phenol is sequentially hydrogenated to cyclohexanone and cyclohexanol, and the latter is selectively dehydrated and dehydrogenated to benzene over multi-functional metal and acid sites. Besides, the side-reactions for hydrogenation of benzene, ethyl-benzene, and PEB are blocked (red lines), as well as the hydrogenolysis of $C_{aromatic}$-O bond is fully suppressed. It can be also concluded that a proper hydrogen pressure (8 bar) guarantees the selective $C_{aliphatic}$-O bond cleavage of PEB (k_1), the rate of phenol hydrogenation (k_2), and cyclohexene dehydrogenation (k_4) (Scheme 3). In addition, a relative high temperature (240 °C) is also an important factor for maintaining the high selectivity of $C_{aliphatic}$-O bond cleavage (k_1), as well as balancing the rates of phenol hydrogenation (k_2), cyclohexanol dehydration (k_3), and finally maximizing the yield for cyclohexene dehydrogenation to benzene (k_4).

Exploration of individual steps phenol and cyclohexanol reactions in tandem steps of PEB hydrodeoxygenation

During PEB hydrodeoxygenation, the crucial step of phenol conversion comprises of individual steps of phenol and

cyclohexanol HDO. The separate kinetics for these two reactions with Ru/SZ are conducted at 240 °C in presence of 8 bar H_2 (Figs. 5a and 5b). The kinetics of phenol conversion (Fig. 5a) demonstrated that the primary products were cyclohexanone and cyclohexanol with a rate of 96 mmol·g^{-1}·h^{-1}, while benzene and cyclohexane occurred as the secondary products. This indicates that benzene is not formed by direct hydrogenolysis of phenol, but via the sequential route of phenol hydrogenation to cyclohexanol, cyclohexanol dehydration to cyclohexene, and then cyclohexene dehydrogenation to benzene. After a reaction time of 100 min., the benzene yield reached at ca. 67%. On the other side, the kinetics on cyclohexanol conversion (Fig. 5b) revealed that it was primarily converted to cyclohexene by dehydration with a rate of 23 mmol·g^{-1}·h^{-1}, while benzene and cyclohexane were shown to be the secondary products.

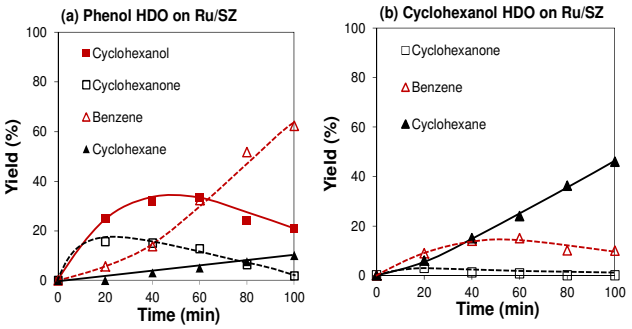

Figure 5. Product distributions of (a) phenol and (b) cyclohexanol HDO over Ru/SZ in water as a function of time. General conditions: H_2O (100 mL), 240 °C, H_2 (8 bar), stirring at 650 rpm. (a) phenol (0.5 g), Ru/SZ (5 wt%, 0.05 g), (b) cyclohexanol (0.5 g), Ru/SZ (5 wt%, 0.10 g).

a.

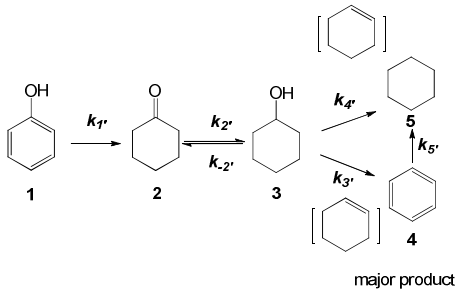

b.

$$\frac{dc_1}{dt} = -k_{1'} \times c_1$$
$$\frac{dc_2}{dt} = k_{1'} \times c_1 - k_{2'} \times c_2 + k_{-2'} \times c_3$$
$$\frac{dc_3}{dt} = k_{2'} \times c_2 - k_{3'} \times c_3 - k_{4'} \times c_3 - k_{-2'} \times c_3$$
$$\frac{dc_4}{dt} = k_{3'} \times c_3 - k_{5'} \times c_4$$
$$\frac{dc_5}{dt} = k_{4'} \times c_3 + k_{5'} \times c_4$$

c.

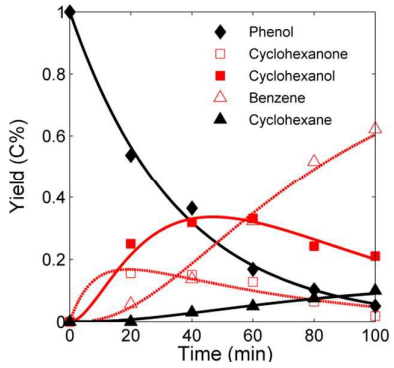

d.

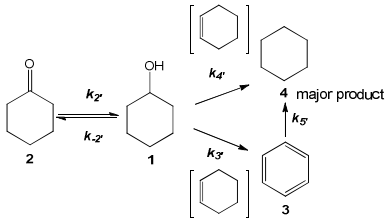

e.

$$\frac{dc_1}{dt} = -k_{-2'} \times c_1 - k_{3'} \times c_1 - k_{4'} \times c_1 + k_{2'} \times c_2$$
$$\frac{dc_2}{dt} = k_{-2'} \times c_1 - k_{2'} \times c_2$$
$$\frac{dc_3}{dt} = k_{3'} \times c_1 - k_{5'} \times c_3$$
$$\frac{dc_4}{dt} = k_{4'} \times c_1 + k_{5'} \times c_3$$

f.

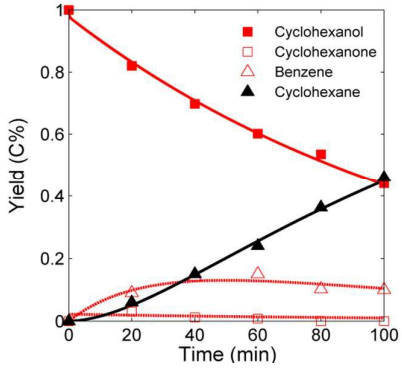

Figure 6. (a) Reaction steps in phenol HDO over Ru/SZ, (b) individual reaction equations in the reaction network of phenol HDO, (c) the fitted curves for phenol HDO over Ru/SZ, (d) reaction steps in cyclohexanol HDO over Ru/SZ, (e) individual reaction equations in the reaction networks of cyclohexanol HDO, and (f) the fitted curves in cyclohexanol HDO over Ru/SZ.

Based on the observation and analysis, the routes for phenol and cyclohexanol HDO are described at Fig. 6a and Fig. 6d, respectively. The former reaction network on phenol (Fig. 6a) illuminates that with respect to phenol HDO, hydrogenation starts as the primary step forming sequential cyclohexanone ($k_{1'}$) and cyclohexanol ($k_{2'}$), afterwards cyclohexanol is dehydrated to cyclohexene (not observed due to the fast sequential steps), and cyclohexene is finally dehydrogenated to target benzene ($k_{3'}$) or hydrogenated to cyclohexane ($k_{4'}$). Meanwhile, a part of benzene is hydrogenated to cyclohexane additionally ($k_{5'}$). The network on cyclohexanol (Fig. 6b) demonstrates that cyclohexanol is dehydrated (k_3, and k_4,) or dehydrogenated (k_2, and k_{-2},) as the primary step, and the dehydrated product cyclohexe67ne is then (k_4,) dehydrogenated to benzene (k_3,) or hydrogenated to cyclohexane. The individual reaction equations in two reaction networks of phenol and cyclohexanol are displayed in Fig. 6b and Fig. 6e.

The fitting curves for the individual steps of phenol and cyclohexanol HDO by the MATLAB software are plotted in Fig. 6c and Fig. 6f, and the individual fitted values are compiled at Table 6. The fitted data for phenol HDO showed that the primary steps of hydrogenation were fast at 0.57 $g^{-1}\cdot min^{-1}$ ($k_{1'}$) and 2.34 $g^{-1}\cdot min^{-1}$ ($k_{2'}$) for producing cyclohexanone and cyclohexanol. The produced cyclohexene from cyclohexanol dehydration followed the selective dehydrogenation route ($k_{3'}$ = 0.30 $g^{-1}\cdot min^{-1}$) in compared to a relatively slow rate for further hydrogenation ($k_{4'}$ = 0.074 $g^{-1}\cdot min^{-1}$) at selected conditions (240 °C, 8 bar H_2). In addition, the hydrogenation of benzene to cyclohexane was not detected ($k_{5'}$ = 0 $g^{-1}\cdot min^{-1}$). The relative large value of $k_{3'}$ together with small values of $k_{4'}$ and $k_{5'}$ indicates that the benzene formation (with a few cyclohexane) is quite selective.

Table 6. Fitted values for the individual steps in phenol and cyclohexanol HDO (unit: $g^{-1}\cdot min^{-1}$).

Steps / Reactant	$k_{1'}$	$k_{2'}$	$k_{-2'}$	$k_{3'}$	$k_{4'}$	$k_{5'}$
(a) phenol	0.57	2.3	0.49	0.30	0.074	0
(b) cyclohexanol	-	70.4	1.60	0.002	0.080	0.40

[a] The conditions are the same as those noted in Figure 5.

By contrast, with respect to the cyclohexanol HDO, firstly the large $k_{2'}$ (70.39 $g^{-1}\cdot min^{-1}$) and small $k_{-2'}$ (1.60 $g^{-1}\cdot min^{-1}$) suggests that dehydrogenation to cyclohexanone occurs in an almost negligible extent. Second, the forty times higher of $k_{4'}$ (cyclohexene to cyclohexane, 0.080 $g^{-1}\cdot min^{-1}$) compared to $k_{3'}$ (cyclohexene to benzene, 0.002 $g^{-1}\cdot min^{-1}$) implies that the final cyclohexane rather than benzene is dominantly formed. Meanwhile, the presence of $k_{5'}$ (0.40 $g^{-1}\cdot min^{-1}$) demonstrates that benzene is partly hydrogenated to cyclohexane.

It should be addressed that the route from cyclohexene

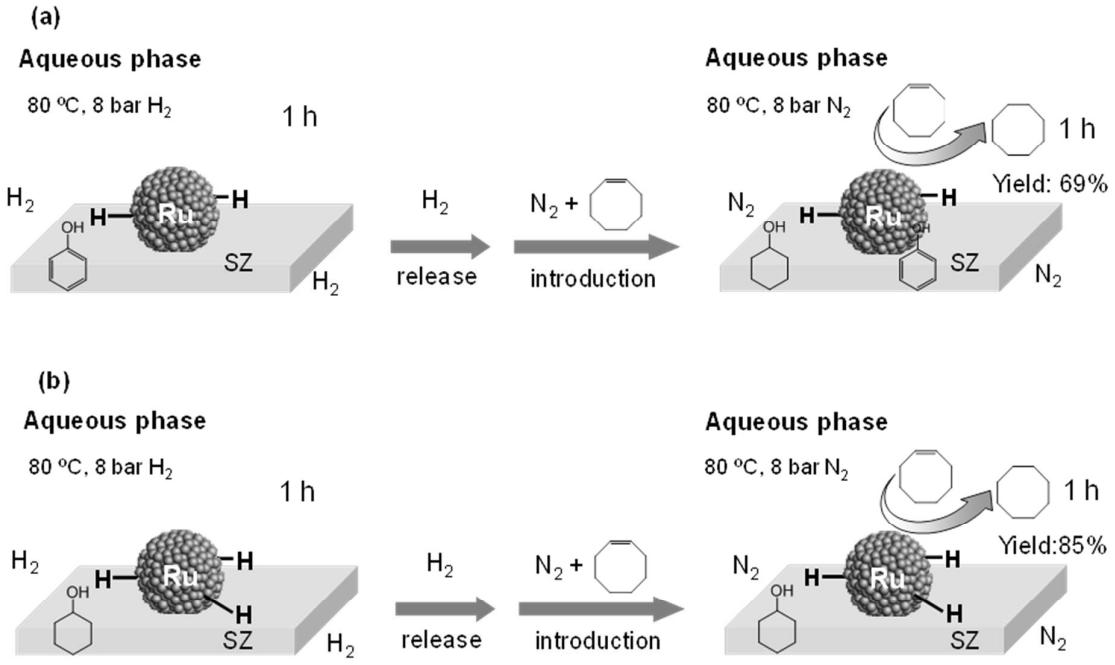

Figure 7. Representative figures for testing the adsorbed surface H· on Ru/SZ (use cyclooctene hydrogenation as the model reaction) after reaction with (a) phenol and (b) cyclohexanol. The initial reaction starts with phenol or cyclohexanol hydrogenation in the sealed autoclave, conditions: reactant (5.0 g), Ru/SZ (5 wt.%,1.0 g), H_2O (100 mL), 80 °C, 8 bar H_2, 1 h, stirring at 650 rpm. Subsequently the hydrogen is released, and the additional nitrogen (8 bar) and cyclooctene (0.10 g) are introduced into the sealed autoclave for reacting for 1 h.

to benzene plays a more crucial role for phenol HDO ($k_{3'}$ = 0.30 $g^{-1}\cdot min^{-1}$) than that for cyclohexanol HDO ($k_{3'}$ = 0.002 $g^{-1}\cdot min^{-1}$), and in an accordance, the cyclohexane yield is more favored from cyclohexanol ($k_{4'}$ = 0.080 $g^{-1}min^{-1}$) than that from phenol ($k_{4'}$ = 0.074 $g^{-1}min^{-1}$) at identical conditions. The plausible reason for attributing to such difference is that the surface adsorbed H· is much fewer during phenol conversion, which will be beneficial for the dehydrogenation step of the formed important intermediate cyclohexene.

To prove this hypothesis, we design the following experiments (Figure 7). The initial reaction started with phenol or cyclohexanol hydrogenation in the sealed autoclave over Ru/SZ in water at 80 °C in presence of 8 bar H_2 for 1 h. Then hydrogen was released, which means that merely the surface adsorbed H· on Ru/SZ is reserved in the reactor. Subsequently nitrogen and cyclooctene were co-introduced and they reacted with the treated Ru/SZ at 80 °C for 1 h. The detected results demonstrated that in the formed case after phenol reaction, the yield of cyclooctene hydrogenation reached 69%. By contrast, in the latter the cyclooctene hydrogenation yield attained much higher at 85% in presence of N_2, evidencing that the surface H· of Ru/SZ possessed lower concentrations of H· after phenol reaction. This supports the observed result that more benzene is formed from phenol conversion, since fewer H· is remained on the surface of Ru/SZ for contributing to a selective dehydrogenation pathway ($k_{3'}$).

Conclusions

A novel route is established for one-pot quantitative hydrodeoxygenation of PEB to benzene and ethyl-benzene over Ru/SZ in aqueous phase. The newly designed approach consists of four consecutive steps of cleavage of $C_{aliphatic}$-O bond of PEB to C_6 phenol and C_8 ethyl-benzene (1), sequential hydrogenation of phenol to cyclohexanol (2), dehydration of cyclohexanol to cyclohexene (3) and final dehydrogenation of cyclohexene to benzene (4). Compared to Ru/SZ, Pd/SZ catalyzes high C-O bond cleavage (k_1) but fails in the sequential phenol hydrogenation, while Pt/SZ exerts slow rates in the primary ether cleavage step.

With the selected Ru/SZ catalyst in the aqueous system, the low hydrogen pressure guarantees the selective $C_{aliphatic}$-O bond cleavage of PEB (k_1), while a too low hydrogen pressure decreases the rate of phenol hydrogenation (k_2), and thus, suppresses the sequential cyclohexanol dehydration (k_3) and cyclohexene dehydrogenation (k_4). A proper pressure-sized H_2 (8 bar) is optimized to ensure the proper rates for four consecutive cascade steps. Moreover, a relative high temperature (240 °C) is also an important factor for maintaining the high selectivity of $C_{aliphatic}$-O bond cleavage, as well as balancing the rates of phenol hydrogenation, cyclohexanol dehydration, and finally maximizing the yield for cyclohexene dehydrogenation to benzene. In addition, the side-reactions for hydrogenation of benzene, ethyl-benzene, and PEB, as well as hydrogenolysis of $C_{aromatic}$-O bond are fully blocked via manipulating the temperatures and pressures.

The separate kinetics experiment on phenol HDO demonstrates that benzene is formed *via* dehydrogenation of the intermediate of cyclohexene (from cyclohexanol dehydration), but not via the direct hydrogenolysis route. In addition, the comparison of phenol and cyclohexanol HDO manifests that fewer surface adsorbed H· on the Ru/SZ (after phenol reaction) leads to a more selective route for benzene formation (step 4), as verified by the model reaction of cyclooctene hydrogenation with the used Ru/SZ in presence of N_2.

Acknowledgements

We are grateful to the financial supports from the Recruitment Program of Global Young Experts (Thousand Youth Talents Plan), National Natural Science Foundation of China (Grant No: 21573075), and Shanghai Pujiang Program PJ1403500.

Notes and references

1. a) J. Zakzeski, P. C. A. Bruijnincx, A. L. Jongerius, and B. M. Weckhuysen, *Chem. Rev.* 2010, **110**, 3552-3599; b) G. W. Huber, S. Iborra, and A. Corma, *Chem. Rev.* 2006, **106**, 4044-4098; c) A. Corma, S. Iborra, and A. Velty, Chem. Rev. 2007, **107**, 2411-2502; d) M. Stocker, *Angew. Chem. Int. Ed.* 2008, **47**, 9200-9211; e) M. Saidi, F. Samimi, D. Karimipourfard, T. Nimmanwudipong, B. C. Gates, and M. R. Rahimpour, *Energy Environ. Sci.* 2014, **7**, 103-129.
2. F. S. Chakar, A. J. Ragauskas, *Ind. Crops Prod.* 2004, **20**, 131.
3. Y. R. Luo, In Comprehensive Handbook of Chemical Bond Energies; CRC Press: Boca Raton, FL, 2007.
4. a) Q. Song, F. Wang, and J. Xu, *Chem. Commun*. 2012, **48**, 7019-7021; b) Q. Song, F. Wang, and J. Xu, *Energy Environ. Sci.* 2013, **6**, 994-1007; c) X. Wang, and R. Rinaldi, *ChemSusChem* 2012, **5**, 1455-1466; d) A. L. Jongerius, P. C. A. Bruijnincx, and B. M. Weckhuysen, *Green Chem*. 2013, **15**, 3049-3056.
5. P. F. Britt, A. C. Buchanan, M. J. Cooney, and D. R. Martineau, *J. Org. Chem.* 2000, **65**, 1376-1389.
6. S. Jia, B. J. Cox, X. Guo, Z. C. Zhang, and J. G. Ekerdt, *ChemSusChem*, 2010, **3**, 1078-1084.
7. a) E. Adler, J. M. Pepper, and E. Eriksoo, *Ind. Engineering Chem*, 1957, **49**, 1391-1392; b) T. J. McDonough, 1992, *Tappi J*. **76**, 186-193.
8. P. F. Britt, M. K. Kidder, and A. C. Buchanan Iii, *Energy Fuels*, 2007, **21**, 3102-3108.
9. A. G. Sergeev, and J. F. Hartwig, *Science* 2011, **332**, 439-443;
10. Y. L. Ren, M. Tian, X. Z. Tian, Q. Wang, H. T. Shang, J. J. Wang, and Z. C. Zhang, *Catal. Commun.* 2014, **52**, 36-39;
11. J. M. Nichols, L. M. Bishop, R. G. Bergman, and J. A. Ellman, *J. Am. Chem. Soc*. 2010, **132**, 12554-12555.

12. Y. L. Ren, M. J. Yan, J. J. Wang, Z. C. Zhang, and K. S. Yao, *Angew. Chem. Int. Ed*. 2013, **52**, 12674-12678.
13. a) J. Zhang, J. Teo, X. Chen, H. Asakura, T. Tanaka, K. Teramura, and N. Yan, *ACS Catal*. 2014, **4**, 1574-1583; b) J. Zhang, H. Asakura, J. Rijn, J. Yang, P. Duchesne, B. Zhang. X. Chen, P. Zhang, M. Saeys, and N. Yan, *Green Chem*. 2014, **16**, 2432-2437.
14. J. He, C. Zhao, and J. A. Lercher, *J. Am. Chem. Soc*. 2012, **134**, 20768-20775.
15. C. Zhao, and J. A. Lercher, *Angew. Chem. Int. Ed*. 2012, **51**, 5935-5940.
16. a) W. Zhang, J. Z. Chen, R. L. Liu, S. P. Wang, L. M. Chen, and K. G. Li, *ACS Catal*. 2014, **2**, 683-691; b) C. Zhao, and J. A. Lercher, *ChemCatChem* 2012, **4**, 64-68; c) H. J. Xu, K. C. Wang, H. Y. Zhang, L. H. Hao, J. L. Xu, and Z. M. Liu, *Catal. Sci. Technol*. 2014, **4**, 2658-2663; d) C. Zhao, S. Kazacov, J. He, and J. A. Lercher, *J. Catal*. 2012, **296**, 12-23; e) C. Zhao, Y. Yu, A. Jentys, and J. A. Lercher, *Appl. Catal. B* 2013, **132-133**, 282-292; f) Q. Song, J. Cai, J. Zhang, W. Yu, F. Wang, and J. Xu, *Chin. J. Catal*. 2013, **34**, 651-658.
17. D. J. Rensel, S. Rouvimov, M. E. Gin, and J. C. Hicks, *J. Catal*. 2013, **305**, 256-263.
18. B. Huang, L. Yan, M. Chen, Q. Guo, and Y. Fu, *Green Chem*. 2015, **17**, 3010-3017.
19. Z. Luo, Y. M. Wang, M. Y. He, and C. Zhao, *Green Chem.* 2015, DOI: 10.1039/C5GC01790D.

Table of Content: